

Oscillatory Fracture Paths in Thin Elastic Sheets: When geometry rules the fracture path

P.M. Reis, B. Roman
PMMH, UMR 7636 CNRS,
Ecole Supérieure de Physique et de Chimie Industrielles
Paris, France

B. Audoly
LMM, UMR 7607 CNRS
Université Pierre-et-Marie-Curie, Paris 6
Paris, France

ABSTRACT

We report a novel mode of quasi-static oscillatory crack propagation when a cutting tool is driven through a thin polymer film [6,7]. In our experiments, for tools with a large enough width, the crack tip follows a highly periodic path, leaving behind a striking oscillatory pattern. Taking into account the separation of the film's bending and stretching energies and using classical fracture theory, we propose a geometrical model that accurately reproduces the behavior observed experimentally. Numerical integration of our geometrical rules accurately reproduces both the shape of the fracture pattern and the detailed time evolution of the propagation of the crack tip [16].

Introduction

A fascinating problem in fracture theory concerns the prediction of the crack path and the associated instabilities: when a piece of material breaks, what determines the shape of the resulting pieces? Within the physics community, there has been a recent upsurge of interest in this question. For example, an oscillatory instability occurs in quasi-static propagation of cracks in thermally quenched strips of silicon and glass [1]. This simple experimental system has stimulated a number of theoretical and numerical studies [2] Another instability has been observed when a bi-axially strained thin rubber sheet is pierced and the crack propagates dynamically [3], the underlying mechanisms of which remains unclear.

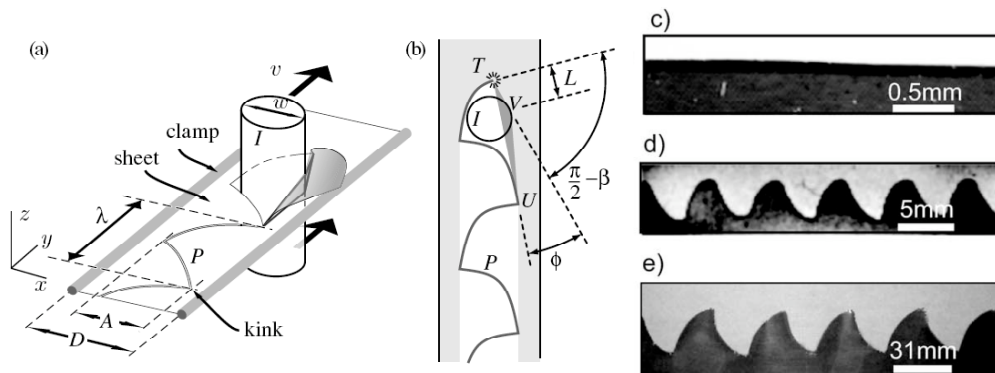


Figure 1. (a) Schematic of an oscillatory path, P , obtained when a cutting tool, I , is driven at constant velocity, v , through a thin polymer film clamped at two of its lateral boundaries. λ and A are the wavelength and amplitude of the pattern, respectively. (b) Our 2D model divides the film into three regions: the *soft region* (white) where the presence of the tool I is accommodated by mere bending of the film, the *active region* (TVU) (dark grey) where of the elastic energy is stored and the *outer region* (light grey). (c-e) Edge of the sheet as seen from above (polypropylene $27\mu\text{m}$ thick) for three cutting tip widths: c) $w=0.15\text{mm}$ (straight path), d) $w=5\text{mm}$ (oscillatory path), e) $w=31\text{mm}$ (oscillatory path). White rectangles are scale bars.

We have studied, both experimentally [6] and theoretically [16], cracks propagating in thin elastic films. Previous studies of cracks in thin plates were concerned with the ductile limit [4], which is relevant in the engineering context of ship plating due to cutting, tearing or bending during collision or grounding [5]. Here, we focus on the opposite limit of brittle thin films. This limit is relevant for the analysis of a novel type of oscillatory crack instability that we have recently reported [6,7,8]. In our experiments, an object, which we denote by *cutting tool*, is perpendicularly driven through a thin polymer sheet held along its lateral boundaries, that progressively cuts the material as it advances [6,7]. For large enough cutting tool widths, the crack follows a well defined and highly reproducible oscillatory path that spans a wide range of length scales.

The experiments

We have performed experiments with thin sheets of different polymeric materials in a range of thicknesses and have investigated the dependence of the resulting fracture paths on the width of the cutting tool. A schematic diagram of the apparatus is presented in Fig1a) and b). It consists of a thin flat sheet (dimensions ranging from $6 \times 60 \text{mm}$ to $120 \times 500 \text{mm}$) clamped along its lateral boundaries and mounted on a linear translation stage. This stage was driven at constant speed, v , towards a fixed object, the *cutting tool*, which could have either rectangular or cylindrical profile, with a variety of widths ($0.05 \text{mm} \leq w \leq 60 \text{mm}$). A camera was mounted directly above the apparatus such that the propagating crack was imaged in the cutting tool's frame of reference.

The sheet was initially prepared with a notch on one of its side boundaries to position and initiate the crack. Both bi-oriented polypropylene and cellulose acetate thin sheets were investigated, with thicknesses ranging between 25 and $130 \mu\text{m}$. The sheet's Young's modulus and fracture energy were measured to lie within the ranges $Y=1\text{-}2 \text{GPa}$ and $\Gamma=2\text{-}5 \text{kJm}^{-2}$, respectively. Although polymeric, these materials are brittle since they have been severely stretched when processed into thin sheets. As a result, they undergo minimal plastic deformation during fracture propagation but, being thin, can sustain large bending without crack initiation. This explains why they are widely used in the packaging industry (resistant but easy to tear once a notch is started). The oscillatory paths discussed below were not observed in ductile materials.

As the thin sheet is forced through the fixed tip, the material is cut, leaving behind a well defined and highly reproducible path. For large enough cutting tools, the resulting path is oscillatory, two examples of which, for significantly different sizes of the cutting tool, are shown in Fig.1d) and e). In this oscillatory regime, the non-sinusoidal oscillatory paths resembles a series of shark fins; the fracture path is made up of smooth curves connected by sharp *kinks*. However, and as one would expect, for thin enough objects, the path left behind the cutting tool is straight; Fig. 1c). Our results point to a new instability in the fracture of thin polymer films from straight to oscillatory patterns, as the size of the cutting tool is increased which was discussed in more detail in [6]. We shall now focus mainly on the regime well above threshold.

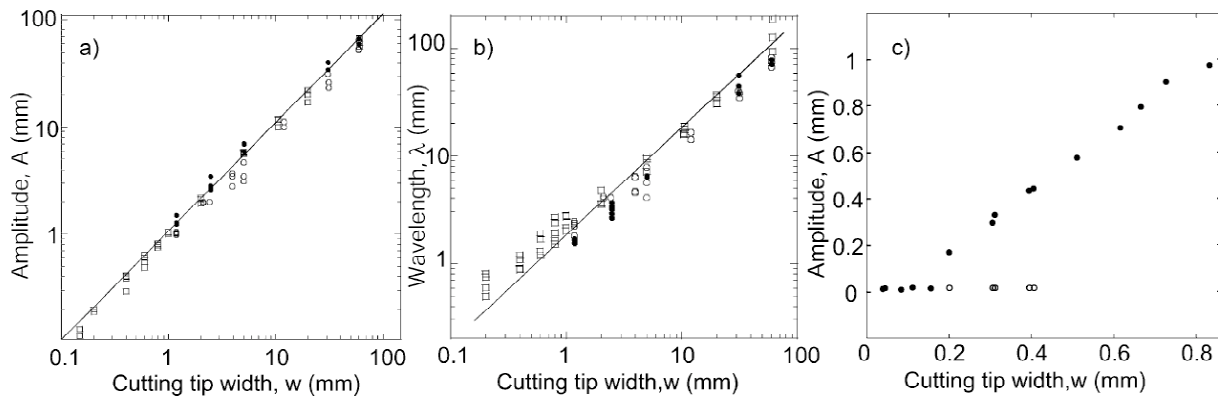


Figure 2. Log-log plots of the (a) peak-peak amplitude, A , and (b) wavelength, λ , of the oscillations as a function of tip width w for various materials and thicknesses (polypropylene $25, 53 \mu\text{m}$: open symbols, cellulose acetate $100, 130 \mu\text{m}$: closed symbols), and for both cylinders (\odot) and rectangular blades (\square). Amplitude and wavelength fall on slope 1 lines, over a range of almost 3 decades. The straight lines represent the best linear fits with slope 1. c) Peak-to-peak amplitude of paths for various cutting tip widths (with rectangular blades), showing the transition between the straight and oscillatory states. Open symbols (\odot) correspond to regions of bi-stability where both oscillatory and straight paths can be observed.

As shown in Fig. 2a,b), we find that both the amplitude A and wavelength λ of the oscillatory paths depend linearly on the width of the cutting tool in this regime, over almost three decades. This linear dependence is valid for a variety of materials and thicknesses. We have also checked, for a fixed tip size $w=2\text{mm}$, that the pattern is independent of the sheet's width, D , within $3.3w < D < 21w$. This feature is *a priori* surprising since one could have thought of D as one of the natural length scales in the problem.

The linear dependence of A and λ on w discussed above breaks down in the vicinity of the transition region between straight and oscillatory paths. In these regions the sheet can no longer be considered thin relative to the cutting tool and the plate bending and stretching energies become of the same order of magnitude. For the transition experiments we have used fine rectangular blades (precision feeler gauges) in the range $0.0375 < w < 0.8\text{mm}$. At this lengthscales the imaging was done with a microscope with a 2x objective. As shown in the plot of Fig. 2c), a clear transition is observed, from a straight crack to an oscillatory regime, as w was incrementally increased. Above a critical cutting tool width, w_c , the amplitude of the oscillatory paths scales linearly with w , as discussed above. Above the transition point, in the vicinity of w_c , there is a region of bi-stability where both straight and oscillatory paths could be observed.

A geometrical model for oscillatory fracture

This simple experimental scaling law, together with the robustness of this instability, suggests that a simple underlying mechanism is at stake. We now show that the classical equation for elastic plates and for crack propagation can be reduced to a simple set of geometrical rules, which explain the experimentally observed crack behavior in thin brittle films mentioned above. Following a common approach in fracture theory, we first calculate the elastic energy of the system, taking into account the possible large out-of-plane deformations of the film induced by the cutting tool. Secondly, we apply Griffith's criterion of propagation of the crack tip.

Deformations of thin films satisfy a set of nonlinear partial differential equations, such as the Föppl–von Kármán equations [9], which makes the description of fracture of thin sheets a challenging endeavor. Fortunately, the following remarks make it unnecessary to resort to the full equations. In the limit of small film aspect ratio, $h/D \ll 1$, (typically $h/D \sim 10^{-3}$ in the experiments), the elastic energy of a film decouples into a bending term, associated with curvature, and a stretching term, associated with longitudinal extension [10]. In thin films ($h \ll D$), the bending energy is formally negligible in front of the stretching one. This suggests that the driving forces for crack propagation lie in in-plane stretching [11]: the bending energy can be neglected, this way allowing large out-of-plane deformations of the film. This affects the repartition of tensile stresses in a manner that we now investigate.

Consider a cylindrical cutting tool I , and a partial crack path P in the sheet. We call the soft zone the region shown in white in Fig. 1(b), which is mathematically defined as the convex hull [12] of the crack path. This soft zone has the particular mechanical property that, as long as the projection of the cutting tool onto the film plane remains fully contained within this zone, the sheet merely bends away, with negligible stretching, to accommodate its presence. The resulting elastic energy is pure bending and, as stated before, is insufficient to make the crack propagate.

In contrast, when the projection of the cutting tool moves beyond one of the boundaries of the soft zone, as in Fig. 1(a), the film is stretched and stores a substantial amount of elastic energy. In Fig. 1(a), the flap with large out-of-plane deformation is connected to the plane of the film along a sharp fold. It is important to note that this fold is pushed upon by the cutting tool and, as a result, is stretched. In the projection onto the film plane [see Fig. 1(b)] this stretching is apparent as the initially straight segment TU becomes a broken line TVU . Any point initially located inside the region TVU will similarly undergo tensile in-plane stresses. Hence, a strain $\varepsilon = L(TUV)/L(TU) - 1 \approx \phi^2/2$ develops in the film, where $L(\cdot)$ denotes the length of a broken line. The angle $\phi \ll \pi/2$ is defined by the boundary of the soft zone, TU , and the outmost edge of the cutting tool, V [see Fig. 1(b)]. The triangle TVU , shown in dark gray in Fig. 1(b), is the region of large tensile in-plane strain which we call the active region, denoted by $A(P, I)$.

We claim that the tensile stresses concentrated in this active region are the driving force for crack propagation. The elastic energy of the film can be estimated as,

$$E(P, I) = Eh \iint_{A(P, I)} dx dy \varepsilon^2(x, y) \approx \frac{YhL^2\phi^5}{40} \quad (1)$$

where the integration is done over the active region $A(P, I)$, x and y are the coordinates along the plane of the film, L is the distance between the crack tip and the cutting tool, and Y is the Young's modulus of the film. An order of magnitude estimation

follows by noting that the tensile in-plane strain inside the active region, $\varepsilon(x,y)$ is of order ϕ^2 and the prefactor 1/40 can be obtained with a more detailed estimate of the stress distribution in this active region.

To address the propagation of the crack tip, we now apply Griffith's criterion [13] which is a balance between the elastic energy stored in the material and that dissipated near crack tip at the microscopic level (by atomic or molecular bonds breaking, by nucleation of defects, etc.). These dissipative processes can collectively be taken into account by introducing an overall effective toughness Γ , with dimensions of surface tension. Hence, any advance of the crack tip by δl dissipates an energy $\Gamma h \delta l$. This toughness, Γ , is a function of the material considered and may also depend on the type of loading at the crack tip but, here, we make the simplifying assumption that Γ is constant throughout the cutting process.

By balancing [14] the release rate of elastic energy, $\delta E / \delta l \approx (\delta E / \delta f) \delta \phi / \delta l$, with the rate of energy dissipation per unit of new crack length, Γh , and by further noticing that $\delta \phi / \delta l$ is given by geometry as $1/L$, we obtain the following propagation criterion from the energy estimation in Eq. (1):

$$\frac{\delta E}{\delta l} \geq \Gamma h \Rightarrow \phi \geq \alpha \quad \text{with} \quad \alpha = \left[\frac{8\Gamma}{YL} \right]^{1/4} \quad (7)$$

Here, α reflects the fracture properties of the material, while ϕ measures the penetration of the tool into the film. When this inequality is satisfied, there is enough energy available for the crack to propagate, otherwise it remains at rest. The weak dependence on L with a power 1/4 makes it a good approximation to replace, in Eq. (2), the variable distance L by the constant cutting tool's width w , both being of the same order of magnitude. Therefore, in the numerical simulations, we take α as a fixed parameter.

The final point to address is the direction of propagation of the crack tip. The classical *principle of local symmetry* assumes that the direction that cancels any mode II loading (in-plane shear) is selected [15]. As discussed above, the driving force for propagation is associated with the stretching of the active zone along the segment $[TU]$. This implies that, near the crack tip, the stresses are essentially opening (mode I), in a direction parallel to the edge of the active zone, (TV) . By the principle of local symmetry, the direction of crack propagation is expected to be approximately perpendicular to this direction: the angle β , defined in Fig. 1(b) as $\pi/2$ minus the angle between the edge $[TV]$ of the active region and the direction of propagation, must therefore be small and is taken to be a constant.

For simplicity, our fracture model has been presented when the cutting tool has a circular cross-section. For an arbitrary section, it can be implemented in the following sequence, which extends the previous construction: (i) compute the convex hull of the crack path, which yields the soft region; (ii) determine the union of the crack path with the cutting tool, and then its convex hull; (iii) calculate the set difference of this convex hull minus the soft region, yielding the active region; (iv) compute the angle ϕ ; (v) if $\phi < \alpha$, propagate the crack along a direction given by β until ϕ decreases back below α . This algorithm predicts the evolution of the crack tip's position using a 2D geometrical construction and elasticity is reflected by the two model parameters α and β .

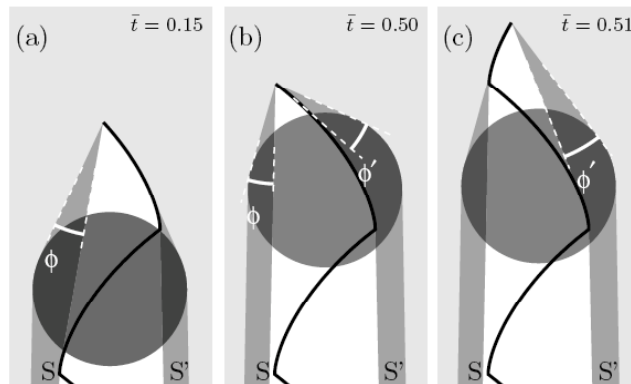


Figure 3. Typical frames from numerical simulations for various dimensionless times $t' = vt/\lambda$: (a) during quasistatic propagation; (b) just before and (c) just after a kink followed by a burst of dynamic propagation. The soft, stretched, and outer regions are shown in white, dark gray, and light gray, respectively. The circle in gray represents the cutting tool. In frame (b), the active region has two components S and S' which define two nonzero angles ϕ and ϕ' at the tip.

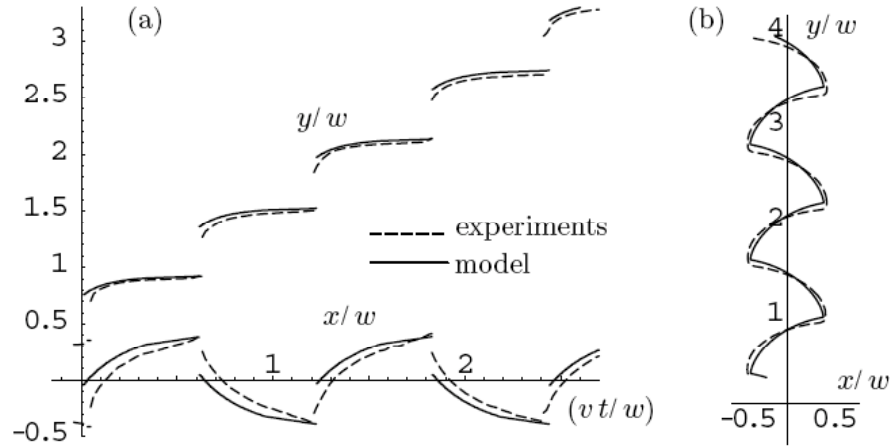


Figure 4. Comparison of crack tip motion from the model and the experiments for a cylindrical cutting tool ($w=20.4\text{mm}$, $h=50\mu\text{m}$, $v=1.2\text{mm}\cdot\text{s}^{-1}$). The model's parameters were $\alpha=0.20$ and $\beta=0.03$. (a) Time series for the crack tip coordinates $x(t)/w$ and $y(t)/w$ as a function of non-dimensionalized tool advance, vt/w . Note the periodic gaps in crack position, corresponding to dynamic propagation. (b) Final pattern in the film plane (x,y) .

We have performed simulations of this geometrical algorithm and found that spontaneous oscillations of the crack are obtained for generic values of the parameters α and β the tool alternatively pushes on either lip of the crack, every change of lip producing a kink. Typical frames from the numerical simulations are shown in Fig. 3. Our model is able to portray the main features of the cracks found experimentally [6,7] and reproduces the detailed time evolution of the crack tip's position. All the material properties of the film are reflected in α and β which, indeed, makes the width of the cutting tool the only relevant length scale. This explains why, within the regime we are considering of $w \gg h$, both the amplitude and wavelength of the crack pattern scale linearly with w and are independent of D , v , and h .

We proceed by comparing the oscillatory cracks obtained from our geometrical model to the experiments reported in [6]. In this comparison, a single type of bi-oriented polypropylene film with $h=50\mu\text{m}$ is used in the experiments (the influence of the film properties has already been documented elsewhere [6,7]). The parameters α and β were therefore set to fixed values, determined once for all by performing a single least squares fit between a series of numerical and an experimental paths corresponding to a variety of indenter shapes (including circular, square, and rectangular cross-sections). This yielded the values $\alpha=0.20$, $\beta=0.03$ which were then used throughout, without further adjustment. Note that the value $\alpha=0.20$ is consistent with an estimate of Eq. (2), for length scales of order 10^{-2}m , using the experimentally measured values of $I=1\text{kJ}/\text{m}^2$ and $Y=1\text{GPa}$ for the particular film we are considering

In Fig. 4 we present the numerical results for a cylindrical tool (solid lines) as a typical example, which we compare against experiments [6] with $w=20.4\text{mm}$ (dashed lines). Excellent agreement is found between the two. In particular, both the kinks and the subsequent bursts of dynamic propagation arise from the simple set of rules (i)–(v). These are, therefore, intrinsic features of the tearing process, which can be understood as follows. Because of the geometry of the system, as the tool advances there are two components to the active zone: to the left, S , and to the right, S' , of the cutting tool (see Fig. 2). At almost all times, only one of these two zones defines a nonzero angle at the crack tip [see Fig. 2(a)] and thus contributes to crack advance. However, when this nonzero angle switches from the left to the right of the crack tip, there is a short period of time (whose duration, relative to a period, is of the order of the small number α) where both angles are nonzero: in the frame of Fig. 2(b), for instance, ϕ has been equal to the critical value α since the previous kink, while ϕ' is rapidly increasing as the tool penetrates into the right hand side rim of the film. The crack bifurcates exactly at the frame of Fig. 2(b), when both angles become equal: $\phi=\phi'=\alpha$. Immediately after this kink, the propagation criterion is overshoot ($\phi'>\alpha$) and a finite advance of the crack is needed for the equality in Eq. (2) to be satisfied ($\phi'=\alpha$), see Fig. 2(c). This dynamic propagation event can be interpreted as the sudden release of the elastic energy stored into region S' between the frames in Figs. 3(a) and 3(b).

Conclusion

We have reported a novel mode of oscillatory crack propagation as a cutting tip is driven through a thin polymer sheet with an associated instability as the cutting tip size is varied. The crack path amplitude and wavelength were found independent of the thickness and lateral width of the sheet, and scale linearly with the size of the object. For cutting tip widths below a critical value, w_c , no oscillatory cracks are observed and the crack path is straight. Although these oscillatory patterns are reminiscent of those observed in thermal quenching experiments [2–4], an important difference is that the oscillation mechanism here arises from a coupling between fracture and the out-of-plane deformations of the sheet. Starting from the principles of elasticity, we have developed a model for the crack patterns in our experiments and showed that the dynamics of fracture is ruled by a simple 2D geometrical construction, based on the interplay between crack propagation and large out-of-plane deformations in the film. This coupling leads to computed crack paths that are in very good agreement with our experiments; both the detailed shape and the motion of the crack tip are accurately reproduced. Geometry, in general, is known to play an important role in the theory of elastic rods, plates, and shells. In the tearing of thin films, geometrical considerations acquire an unprecedented level of importance: to our knowledge, this is the first example where a complex crack motion is entirely ruled by geometry.

References

1. A. Yuse and M. Sano, *Nature (London)* **362**, 329 (1993); O. Ronsin, F. Heslot, and B. Perrin, *Phys. Rev. Lett.* **75**, 2352 (1995); R. Deegan et al., *Phys. Rev. E* **67**, 66209 (2003).
2. B. Yang and K. Ravi-Chandar, *J. Mech. Phys. Solids* **49**, 91 (2001); M. Adda-Bedia and Y. Pomeau, *Phys. Rev. E* **52**, 4105 (1995); H. Henry and H. Levine, *Phys. Rev. Lett.* **93**, 105504 (2004); M. Adda-Bedia and M. Ben Amar, *Phys. Rev. Lett.* **76**, 1497 (1996).
3. R. Deegan, P. Petersan, M. Marder, and H. Swinney, *Phys. Rev. Lett.* **88**, 014304 (2002).
4. E. Sharon and B. Roman, *Nature (London)* **419**, 579 (2002); B. Audoly and A. Boudaoud, *Phys. Rev. Lett.* **91**, 086105 (2003).
5. H. Vaughan, *Nav. Archit.* **97**, 97 (1978); T. Wierzbicky and P. Thomas, *Int. J. Mech. Sci.* **35**, 209 (1993).
6. B. Roman et al., *C. R. Mécanique* **331**, 811 (2003);
7. A. Ghatak and L. Mahadevan, *Phys. Rev. Lett.* **91**, 215507 (2003).
8. B. Audoly, B. Roman, and P. M. Reis, *Phys. Rev. Lett.* **94**, 129601 (2005).
9. L. D. Landau and E. M. Lifschitz, *Theory of Elasticity* (Pergamon, New York, 1959).
10. A. Pogorelov, *Bending of Surfaces and Stability of Shells*, Translation of Mathematical Monographs (American Mathematical Society, Providence, 1988).
11. That bending energy is too small to influence crack propagation can be confirmed by sharply creasing a plastic film between two fingers. This leads to permanent marks (hence much higher curvatures than in our experiments) but does not suffice to break the film.
12. A convex hull is the smallest convex set that contains a given subset, here the crack path P.
13. A. A. Griffith, *Phil. Trans. R. Soc. A* **221**, 163 (1921).
14. In Griffith's criterion, the increment of crack length is virtual and occurs while the tool is stationary. This is analogous to writing a condition of stationary energy, $dE=0$, for virtual changes of state dx of a system at equilibrium.
15. R. V. Goldstein and R. Salganik, *Int. J. Fract.* **10**, 507 (1974).
16. B. Audoly, P.M. Reis and B. Roman, *Phys. Rev. Lett.* **95**, 025502 (2005),